PHYSICAL REVIEW E **92**, 020201(R) (2015)

Mechanical fluctuations suppress the threshold of soft-glassy solids: The secular drift scenario

Adeline Pons,[1] Axelle Amon,[2,*] Thierry Darnige,[1] Jérôme Crassous,[2] and Eric Clément[1]
[1]*PMMH, ESPCI, UMR CNRS 7636; Université Paris 6; and Université Paris 7, 75005 Paris, France*
[2]*Université Rennes 1, Institut de Physique de Rennes, UMR UR1-CNRS 6251, Bâtiment 11A, Campus de Beaulieu, 35042 Rennes, France*
(Received 9 December 2014; revised manuscript received 4 May 2015; published 20 August 2015)

We propose a dynamical mechanism leading to the fluidization by external mechanical fluctuations of soft-glassy amorphous material driven below the yield stress. The model is based on the combination of memory effect and nonlinearity, leading to an accumulation of tiny effects over a long term. We test this scenario on a granular packing driven mechanically below the Coulomb threshold. We provide evidence for an effective viscous response directly related to small stress modulations in agreement with the theoretical prediction of a generic secular drift. We propose to extend this result more generally to a large class of glassy systems.

DOI: 10.1103/PhysRevE.92.020201 PACS number(s): 83.80.Fg, 82.70.Dd, 81.40.Lm, 83.50.−v

Introduction. Numerous amorphous materials such as concentrated suspensions, colloidal glasses, foams, and granular materials share common global features in their mechanical response to shear [1,2]. They are characterized by a yield stress below which the material appears as a solid [3,4]. As this behavior is shared by so many different materials, several conceptual and theoretical frameworks have emerged [5–10] to provide a quantitative basis for the phenomenology of soft-glassy rheology (SGR) above and below the yield stress. Even though many parallel approaches exist, sometimes at a different level of description, they all share either explicitly or implicitly the underlying idea that mesoscopic collective processes triggered by thermal or mechanical activation contribute to the material fluidity. The direct visualization of local plastic events and the associated complex avalanching dynamics is supported by many experimental [11–14] and numerical [15–17] studies. In the solid phase corresponding to a strong dynamical arrest, soft-glassy systems display aging properties manifesting in a slow creep relaxation process [18–21]. Aging properties stem from a remaining thermal activation providing the possibility to cross enthalpic or entropic barriers and progressively set the system into deeper local minima where mechanical solidity is reinforced. The existence of external mechanical noise was also proposed as a substitute for thermal activation. In this sense, the behavior of these amorphous soft-glassy solids is very close phenomenologically to molecular glass formers obtained by thermal quenching [22]. However, the idea that such mechanical noise truly acts as an effective temperature is presently debated [23] and indeed deep differences in the way thermal noise and mechanical fluctuations act in amorphous systems was recently pointed out [24].

In the solid-glassy phase, where the system never reaches thermal equilibrium at the level of experimental times, in addition to the presence of an elastic response, theories have to account for the loss of ergodicity. This is done either by introducing a memory kernel in the soft-glassy rheology [8,21,25] or by providing phenomenologically dynamical relations for an effective fluidity parameter [10,19] suited to render the rheological age of the system and its temporal evolution. Note that the two approaches, not working at the same level of representation, are not necessarily contradictory and in some simple cases explicit connections can even be made [26].

From a practical point of view, even far from the fluidization thresholds, many situations show that vanishingly small perturbations cannot be neglected in the presence of a bias. Since such effects may be cumulated over long times, it becomes problematic when a solid response is expected but uncontrolled mechanical noise would eventually lead to a significant creep. For example, the effect of mechanical noise on soils is of major importance for the long-term stability of structure foundations [27]. It may also play a determinant role in the context of triggering earthquakes [28]. Controlled mechanical fluctuations can also be used as an investigation tool, for example, in superposition rheology [29]. In this instance, understanding the system response to various forcing of different forms and amplitudes, as well as the importance of inherent apparatus wobbling noise, is crucial for an accurate exploitation of the system dynamics. From a theoretical point of view, it has been shown that aging in a glass spin model is interrupted in the presence of a bias [30].

In this Rapid Communication we propose an alternative conceptual picture to understand a fluidization process that a soft-glassy materials may undergo in the solid phase under external mechanical noise. This scenario differs from an activated process and does not require the introduction of an effective temperature. First, theoretical arguments are presented to describe the solid phase where aging and shear rejuvenation processes are both present. Second, an explicit derivation is presented on a generic rheological model. Third, we present experiments on granular packing sheared below the Coulomb threshold and we show that the response to small mechanical modulations is in agreement with the generic predictions of the model. Finally, the result's generality and its application to soft-glassy materials are discussed.

Model. Models aiming at describing yield-stress fluids and amorphous materials in the solid phase need to account for two fundamental features in their dynamics [6,10]: (i) aging of the system with time and (ii) rejuvenation due to shear rate $\dot{\gamma}$. That rejuvenation can be seen microscopically as a local structural reorganization induced by the strain. When an amorphous material is submitted to a cyclic load, after a complete cycle, the system is not back at its initial state [10], which means that the rate of evolution of the variable describing the state of the system has an even dependence on the shear rate $\dot{\gamma}$. Because of

*axelle.amon@univ-rennes1.fr

the different time scales at play in the dynamics (typical time of reorganization compared to the aging time), the description of glassy materials depends on the observation time scale. Choosing this scale can be problematic in creep experiments as the system exhibits no intrinsic time scale. In the presence of stress fluctuations, the macroscopic variables measured are averaged quantities giving the mean long-term behavior. If the system is submitted to stress variations of typical amplitude δ, which is very small compared to the yield stress σ_D, and display a characteristic time $\tau_{\rm vib}$, a pertinent observation time is given by the number of perturbations of amplitude δ necessary to accumulate an equivalent stress of order σ_D: $T_{\rm obs} = \frac{\sigma_D}{\delta}\tau_{\rm vib}$. Because of the positive nonlinear dependence of the rejuvenation term, one can expect a dynamical stack of those perturbations, giving rise, after a time of order $T_{\rm obs}$, to an equivalent stress of order σ_D.

Fluidization as a secular drift. In order to demonstrate simply how this mechanism works, we build on the macroscopic rheological model proposed by Derec *et al.* [10] to understand the rheology of soft-glassy materials. This model was used to analyze aging and nonlinear rheology of pastes [19] and also creeping processes in granular matter [13,20,31]. This generic model introduces a macroscopic phenomenological variable, the *fluidity* defined as the inverse time scale characterizing the material viscoelastic response. To provide a comprehensive analytical understanding of how a steady fluidity can appear below the dynamical yield stress σ_D, we first study the response on the simplest nontrivial form of the model

$$\dot\sigma = G\dot\gamma - f\sigma, \tag{1}$$

$$\dot f = -af^2 + r\dot\gamma^2, \tag{2}$$

where σ is the applied shear stress, $\dot\gamma$ is the shear rate, G is the shear elastic modulus, and $f(t)$ is the fluidity. Dimensionless parameters a and r represent, respectively, aging and shear-induced rejuvenation processes and for clarity and simplicity we consider them as constant. The stationary solutions of those equations depend on the value of the stress compared to the dynamical yield threshold $\sigma_D = G\sqrt{a/r}$. For a constant $\sigma < \sigma_D$, the fluidity f, as well as the shear rate $\dot\gamma$, decreases to 0 as the inverse of time, thus leading to a logarithmic creep process. We consider the case of a mean imposed stress σ_0 below the threshold σ_D combined with a modulation of small amplitude $\delta \ll \sigma_0$, leading to an imposed stress $\sigma(t) = \sigma_0 + \delta\sin(\omega t)$. By construction, the present fluidity model has no time scale. When imposing a modulation, one can study the in-phase and out-of-phase responses [10] over a time of the order of $\tau_{\rm vib} = \frac{2\pi}{\omega}$. Here we aim at understanding the long-term behavior, given by the number of cycles of amplitude δ necessary to build up an equivalent stress of order σ_D: $T_{\rm obs} = \tau_{\rm vib}/\epsilon$, with $\epsilon = \delta/\sigma_D$. The equations are adimensionalized using the following scales: $1/\epsilon\omega$ for time, σ_D for stress, and $\gamma_0 = \sigma_D/G$ for deformation. The adimensionalized variables are written with a tilde, thus yielding the equations $\dot{\tilde\sigma} = \dot{\tilde\gamma} - \tilde f\tilde\sigma$ and $\dot{\tilde f} = -a(\tilde f^2 - \dot{\tilde\gamma}^2)$, with $\tilde\sigma = \tilde\sigma_0 + \epsilon\sin(\frac{\tilde t}{\epsilon})$, which gives

$$\dot{\tilde\gamma} = \cos\left(\frac{\tilde t}{\epsilon}\right) + \tilde f\tilde\sigma_0 + \epsilon\tilde f\sin\left(\frac{\tilde t}{\epsilon}\right). \tag{3}$$

Dynamically, one obtains a two-time system with $T = \tilde t$ the time of observation corresponding to creep (*slow* time) and the modulation time $\tau = \tilde t/\epsilon$ (*fast* time). A multiple-scale perturbation analysis can be done [32] using $\frac{d}{d\tilde t} = \frac{1}{\epsilon}\frac{\partial}{\partial\tau} + \frac{\partial}{\partial T}$ and searching for a solution of the form $\tilde f(\tau,T) = \tilde f^{(0)}(\tau,T) + \epsilon\tilde f^{(1)}(\tau,T) + \cdots$. We then obtain, for $(1-\tilde\sigma_0^2) = O(1)$,

$$\begin{aligned}&\frac{1}{\epsilon}\frac{\partial\tilde f^{(0)}}{\partial\tau} + \frac{\partial\tilde f^{(1)}}{\partial\tau} + \frac{\partial\tilde f^{(0)}}{\partial T} + O(\epsilon)\\ &\quad= -a\left[-\frac{1-\cos 2\tau}{2} + \left(1-\tilde\sigma_0^2\right)(\tilde f^{(0)})^2 + 2\tilde f^{(0)}\tilde\sigma_0\sin\tau + O(\epsilon)\right].\end{aligned} \tag{4}$$

From the leading order $O(\frac{1}{\epsilon})$, one obtains $\frac{\partial\tilde f^{(0)}}{\partial\tau} = 0$, so $\tilde f^{(0)}(\tau,T) = \tilde f^{(0)}(T)$; the envelope is a function of the slow time only. The order $O(1)$ gives

$$\begin{aligned}\frac{\partial\tilde f^{(1)}}{\partial\tau} = &-\frac{d\tilde f^{(0)}}{dT} + a\left[\frac{1}{2} - \left(1-\tilde\sigma_0^2\right)(\tilde f^{(0)})^2\right]\\ &- a\left[2\tilde f^{(0)}\tilde\sigma_0\sin\tau - \frac{\cos 2\tau}{2}\right].\end{aligned} \tag{5}$$

The term $-\frac{d\tilde f^{(0)}}{dT} + a[\frac{1}{2} - (1-\tilde\sigma_0^2)(\tilde f^{(0)})^2]$ on the right-hand side of Eq. (5) does not depend on τ, so its integration would give a term proportional to τ, which would lead to a failure of the expansion over a long time. This term, called the secular term because its effect is seen only after a very long time, thus needs to be canceled for the perturbation analysis to hold (see, e.g., [32]). This leads to the differential equation

$$\frac{\partial\tilde f^{(0)}}{\partial T} = a\left[\frac{1}{2} - \left(1-\tilde\sigma_0^2\right)(\tilde f^{(0)})^2\right]. \tag{6}$$

This equation corresponds to the normal form of a saddle-node bifurcation $\dot x = \mu - x^2$. For $\mu > 0$ the solution $+\sqrt{\mu}$ is the only stable stationary solution. The dimensional expression of the stationary value for the mean fluidity f^* is thus $f^* = \frac{\omega\delta/\sigma_D}{\sqrt{2(1-\sigma_0^2/\sigma_D^2)}}$, which is finite for nonvanishing values of δ, the stress modulation, even when $\sigma_0 \ll \sigma_D$. Consequently, even far below the yield threshold, the long-term behavior tends to create a liquidlike response, with constant mean strain rate $\dot\gamma^{(0)} = \frac{f^*}{G}\sigma_0$ corresponding to a finite effective viscosity

$$\eta = G/f^* = G\sqrt{2\left(1-\frac{\sigma_0^2}{\sigma_D^2}\right)}\frac{\sigma_D}{\omega\delta}. \tag{7}$$

Note that this viscous response is linearly related to the inverse of the stress modulation rate ($R_\sigma = 2\omega\delta/\pi$). In the Appendix we numerically show that secular drift is a robust result that can be applied to a large class of macroscopic rheological models, the essence of the phenomenon being indeed captured by the previous simple case. We also show that the secular drift does not depend on the nature of the stress modulations (see the results for random forcing in the Appendix).

Stress modulation experiments. The generic theoretical outcomes are now tested experimentally on a granular packing under a confinement pressure that sets a scale for the Coulomb dynamical yield stress. Granular materials are often seen as rigorously athermal. Indeed, in most numerical approaches, granular contacts are modeled as elastic repulsive forces

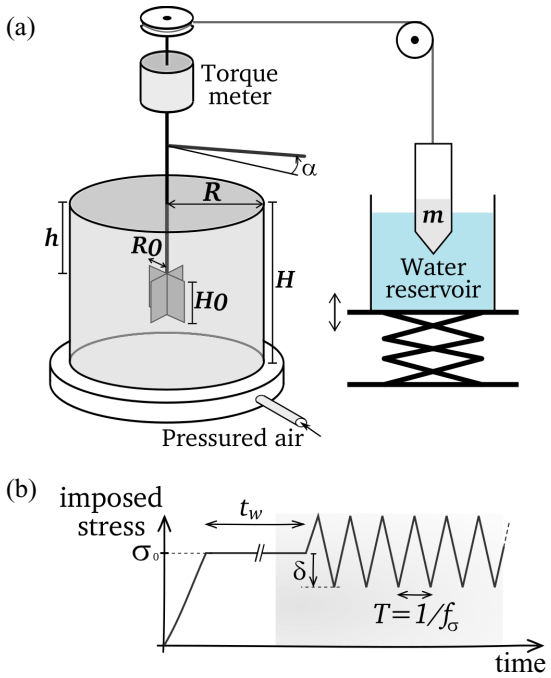

FIG. 1. (Color online) (a) Experimental setup. (b) Imposed stress during an experiment: stress ramp to reach mean stress σ_0, constant stress during t_w, and stress modulation characterized by a frequency f_σ and an amplitude δ.

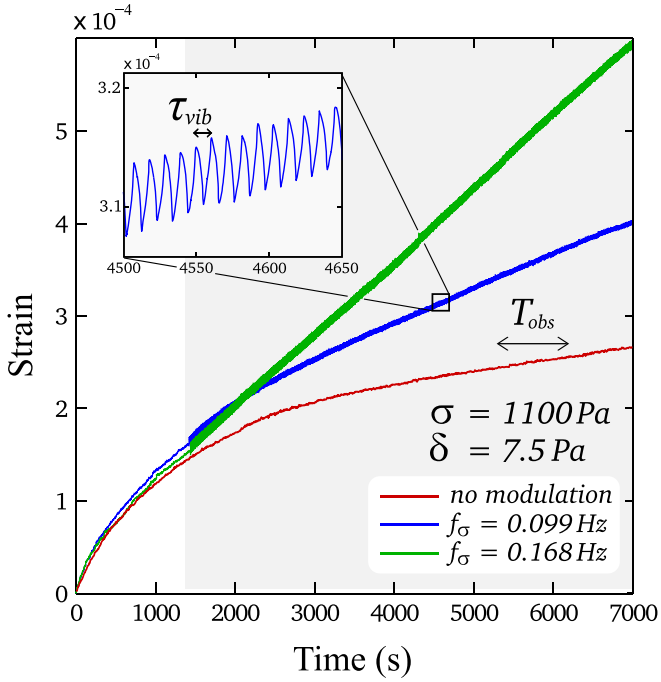

FIG. 2. (Color online) Strain as a function of time for three experiments performed at $\sigma_0 = 1100$ Pa, $\delta = 7.5$ Pa, and various oscillations frequencies. The oscillations start at $t = 1500$ s (gray area).

and a Coulomb solid friction threshold. Consequently, for infinitesimal deformations around a reference state, a granular packing should possess a true elastic response and displays no aging [33]. Note, however, that in the limit of very small if not zero friction the establishment of a linear elastic response under finite shear is questionable [34]. Moreover, for real granular materials, the actual pressures at contact are generically high and contacts may creep plastically. Therefore, the contact status will be intrinsically coupled to a thermally activated process [35]. In addition, the contact status can also be extremely sensitive to the ambient mechanical noise. In fact, real granular packing in the solid phase displays aging and shear rejuvenation that can be modeled directly by Eq. (2) [20]. Moreover, the fluidity variable $f(t)$ was identified experimentally (for shear stresses not too close to the yield stress) as the rate of occurrence of local rearrangements called "hot spots" [13], thus providing an explicit experimental connection with more mesoscopic theories describing structural relaxation processes. As a consequence, experiments on granular packing in the solid phase can be considered to be of general relevance to the class of soft-glassy materials that display similar phenomenology [36].

An experimental key point here is to achieve shear stress modulations around a nominal value without introducing uncontrolled mechanical perturbations. Besides residual external noise, which is always present, even in quiet environments, a substantial source of mechanical noise comes from motorized elements. This is why we designed the experimental system as an Atwood machine. The setup is shown in Fig. 1(a). It consists of a shear cell (radius $R = 5$ cm and height $H = 10$ cm) filled with glass beads of density $\rho = 2500$ kg/m^3 and mean diameter $d = (200 \pm 30)$ μm. A well-defined packing fraction $\phi = 0.605 \pm 0.005$ is obtained by a procedure described elsewhere [20].

Shear is obtained by applying a torque on a four-blade vane ($R_0 = 1.27$ cm, $H_0 = 2.54$ cm) using a mass m suspended from a pulley (vane penetration $h = 5$ cm) [see Fig. 1(a)]. A torque probe measures the applied torque $\mathcal{T}$ and the angle of rotation of the vane α is measured by an induction probe. We define the mean stress and the mean strain as $\sigma = \frac{\mathcal{T}}{2\pi R_0^2 H_0}$ and $\gamma = \frac{\alpha R_0}{R - R_0}$, respectively. Under the conditions of the present experiment, the Coulomb threshold is determined at a value $\sigma_Y = 2300$ Pa. When a constant stress σ_0 smaller than the yield stress is applied on the granular packing, a creep behavior is observed with a logarithmic dependence of the strain with time (red curve of Fig. 2). This behavior was studied in [20] and the fluidity model discussed previously describes accurately the observed response.

By variation of Archimede's forces, a modulation of the applied torque is obtained by vertical oscillatory displacements of a mass m hanging partially in a water tank. The protocol [Fig. 1(b)] is then (i) stress ramp at constant stress rate ($\dot{\sigma} = 5$ Pa/s) up to the desired mean stress value σ_0, (ii) apply constant shear σ_0 for $t_w = 1500$ s, and (iii) modulate the stress around σ_0 for at least 2 h. The modulations are triangular oscillations of amplitude δ and frequency f_σ. Figure 2 shows typical deformations for two experiments performed at the same mean stress ($\sigma_0 = 1100$ Pa) and oscillation amplitude ($\delta = 7.5$ Pa) but for various oscillation frequencies. During the constant stress phase, a slow increase of the deformation $\gamma(t)$

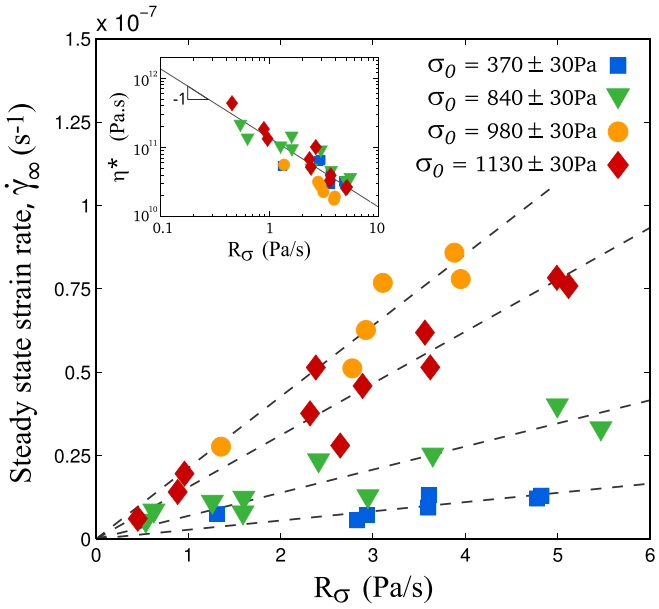

FIG. 3. (Color online) Steady-state strain rate $\dot{\gamma}_\infty$ as a function of modulation stress rate R_σ for four different values of mean stress σ_0. The straight lines are linear fits. The inset shows the normalized viscosity $\eta^* = \eta/\sqrt{1-\sigma_0^2/\sigma_D^2}$ as a function of R_σ with $\sigma_D = 1240$ Pa.

is observed corresponding to the beginning of the logarithmic creep. Then, when submitted to oscillations, the system will transit to a linear creep regime characterized by a constant mean strain rate $\dot{\gamma}_\infty$, which increases with the oscillation frequency. The slope of this linear creep allows us to define an effective viscous response $\eta = \sigma_0/\dot{\gamma}_\infty$. Figure 3 shows the values obtained for the mean strain rate $\dot{\gamma}_\infty$ as a function of the modulation stress rate $R_\sigma = 2\omega\delta/\pi$ for a given value of the applied mean stress σ_0. The observed linear dependences are in agreement with the normalization parameters chosen. Indeed, the finite viscosity that we expect to arise from the modulation should vary as $\eta \propto \frac{1}{\delta\omega}$ [see Eq. (7)], leading to a strain rate $\dot{\gamma}_\infty \propto \omega\delta$. The applied mean stress σ_0 corresponds to an applied shear stress far enough from the dynamical threshold. Experimentally, when this limit is approached one observes a strong increase of the strain rate. The results are then much less reproducible and may be quite sensitive to uncontrolled external perturbations. A collapse of the measurements done at different imposed stress σ_0 can be obtained by plotting $\eta^* = \eta/\sqrt{1-\sigma_0^2/\sigma_D^2}$ as a function of the modulation stress rate R_σ (inset of Fig. 3), in agreement with Eq. (7).

Conclusion. In this Rapid Communication we presented a fluidization pathway that could apply to a large class of soft-glassy materials arrested dynamically in the solid phase. The mechanism requires two generic features: memory effects and nonlinear flow-induced rejuvenation. Under external shear stress and below the yield stress, small fluctuations around the mean shear accumulate tiny irreversible strains over a long time and lead to secular drifts [32] that can be viewed as an effective viscous response. Even though the derivation was explicitly done on a simple macroscopic rheological model, the existence of a secular term yielding a finite material fluidity is a generic feature resulting from any model mixing aging and nonlinear rejuvenation process [36]. The underlying mechanism at work is in principle very different from a thermal activation or any equivalent mechanism accounting for stress fluctuations as an effective temperature [30,37]. In the latter case, the amplitude of the fluctuations must help to overcome a barrier or a threshold. In our case, fluidization stems from a dynamical bifurcation of the rheological equations as a very general feature of a dynamical system hosting processes working at very different time scales. It would be interesting to see how in more sophisticated SGR models with memory kernels accounting for aging [8] the equation's dynamics solved for similar driving conditions would also give a secular drift. Evidence and a quantitative assessment of the effect were provided for a granular packing submitted to controlled stress modulations below the Coulomb threshold. We related quantitatively the effective viscosity to the inverse of the stress modulation rate and have shown that the viscosity decreases significantly when approaching the dynamical threshold. Note that, in spite of resemblances, this phenomenon is *a priori* different from another fluidization process occurring when a granular packing is placed in contact with a fluidized shear band [38,39]. In the latter case, theoretical analysis and numerical simulations show that the induced creeping process comes from a nonlocal stress relaxation from the flowing part to the material bulk [40–43]. The generality of the scenario of mixing two generic features of a glassy system makes it suitable to be tested experimentally on many other practical situations such as colloidal glasses, pastes, clays, and even glass-former molecular systems, which actually may turn out to be of practical importance to assess the stability and reliability of structures strained externally in their environment over very long time scales. Finally, an important question remains about the plastic relaxation modes involved in the material strain in the context of this scenario (localized or extended). This is left for future work [44].

Acknowledgements. E.C., A.P., and T.D. acknowledge the ANR grant Jamvibe-2010 and a CNES-DAR grant. A.P. acknowledges postdoctoral financial support from CNES. A.A. and J.C. acknowledge "action incitative" funding from UR1.

APPENDIX: NUMERICAL SIMULATIONS

1. Comparison of models

In Ref. [10], a general form for the equation governing the fluidity is proposed, coming from a Landau-type expansion

$$\frac{\partial f}{\partial t} = -a\left(1 - \left(\frac{|\sigma|f}{|\dot{\gamma}|}\right)^{\lambda}\frac{|\dot{\gamma}|^{\nu-\epsilon}}{f^{\nu}}\right)f^{\alpha}, \qquad \text{(A1)}$$

where the higher orders of f in the expansion have being dropped because we work in the pasty phase where f is small. We also only study the cases when $\epsilon = 0$ because we want to study a yield-stress fluid (see [10]). The analytical study presented in our Rapid Communication treats the case $(\alpha,\lambda,\nu,\epsilon) = (2,0,2,0)$. Nevertheless, the underlying mechanism that leads to a subthreshold rejuvenation of the fluidity originates from the $|\dot{\gamma}|^{\nu-\lambda}$ term ($\epsilon = 0$), so when $\nu \neq \lambda$,

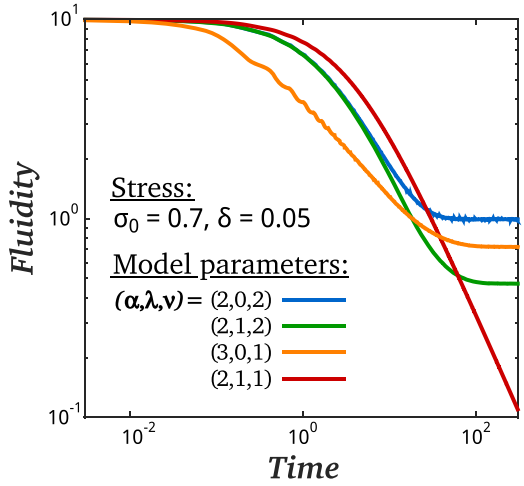

FIG. 4. (Color online) Fluidity as a function of time obtained from the numerical integration of Eq. (A1) for different sets of exponents and subjected to a sinusoidal perturbation ($\sigma_0 = 0.7, \delta = 0.05$).

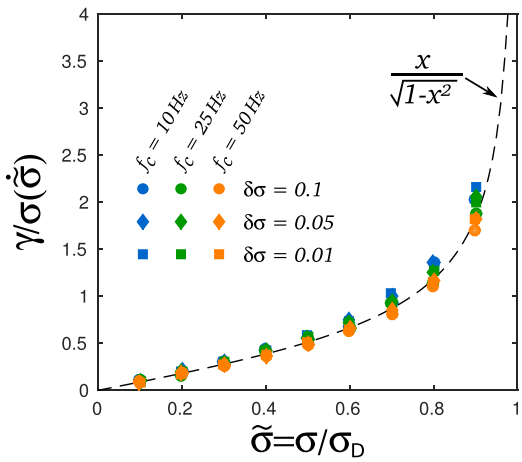

FIG. 5. (Color online) Results of numerical simulation using noise instead of a regular oscillation as a perturbation for $a = 0.1$ and an initial fluidity of $f_0 = 10\ \mathrm{s}^{-1}$: strain rate in the steady state divided by the standard deviation of the stress rate $\sigma(\dot{\tilde{\sigma}})$ as a function of the imposed mean stress normalized by σ_D.

the subthreshold fluidization should always be observed. We demonstrate this by using numerical integrations for different sets of exponents. Figure 4 shows the evolution in time of f for four set of (α,λ,ν) keeping $\epsilon = 0$. We set $a = 1$ and impose a sinusoidal stress ($\sigma_0 = 0.7, \delta = 0.05$).

We obtain a finite fluidity whenever $\nu \neq \lambda$. In contrast, when $\nu = \lambda$ [red curve in Fig. 4, case $(\alpha,\lambda,\nu) = (2,1,1)$], the creep remains logarithmic in the presence of small perturbations because the equation becomes

$$\frac{\partial f}{\partial t} = -a(1 - |\sigma|) f^{\alpha}$$

and we have always $|\sigma(t)| \ll 1$ as the perturbation is well below the threshold. Consequently, no fluidization can be observe as the perturbation is not strong enough to pull the system over the threshold. Varying a or σ does not affect the general behavior of the system as long as $\sigma(t)$ remains below 1.

2. Response to random forcing

We also test numerically the response of the model presented to a stress modulated by random fluctuation. We found that such modulation has the same overall effect as a regular perturbation. Figure 5 shows the results of the numerical integration of Eqs. (1) and (2) using $\sigma(t) = \sigma_0 + \xi(t)$, where $\xi(t)$ is a noise presenting a uniform frequency distribution between 0 and f_c and whose standard deviation equals $\delta\sigma$. A subthreshold fluidization is recovered for all the set of parameters we have tested. By normalizing the strain rate obtained in the steady state by the standard deviation of the stress rate $\sigma(\dot{\tilde{\sigma}})$, we obtain a collapse of the data for $\sigma_0 \ll \sigma_D$. One can note the collapse perfectly in our analytical solution

$$\dot{\gamma}_{\infty} = \frac{\dot{\Sigma}\sigma_0/\sigma_D}{\sqrt{1 - \sigma_0^2/\sigma_D^2}}$$

in which $\dot{\Sigma}$ is a characteristic stress rate. Here $\dot{\Sigma}$ corresponds to the standard deviation of the stress rate for sinusoidal modulations ($\omega\delta/\sqrt{2}$) and random modulations, respectively.

[1] A. J. Liu and S. R. Nagel, Nature (London) **396**, 21 (1998).
[2] L. Berthier, G. Biroli, J.-Ph. Bouchaud, L. Cipelletti, and W. van Saarloo, *Dynamical Heterogeneities in Glasses, Colloids, and Granular Media* (Oxford University Press, Oxford, 2001).
[3] P. Coussot, Q. D. Nguyen, H. T. Huynh, and D. Bonn, Phys. Rev. Lett. **88**, 175501 (2002).
[4] P. C. F. Møller, A. Fall, and D. Bonn, Europhys. Lett. **87**, 38004 (2009).
[5] M. L. Falk and J. S. Langer, Phys. Rev. E **57**, 7192 (1998).
[6] P. Sollich, F. Lequeux, P. Hébraud, and M. E. Cates, Phys. Rev. Lett. **78**, 2020 (1997).
[7] P. Hébraud and F. Lequeux, Phys. Rev. Lett. **81**, 2934 (1998).
[8] S. M. Fielding, P. Sollich, and M. E. Cates, J. Rheol. **44**, 323 (2000).
[9] L. Bocquet, A. Colin, and A. Ajdari, Phys. Rev. Lett. **103**, 036001 (2009).
[10] C. Derec, A. Ajdari, and F. Lequeux, Eur. Phys. J. E **4**, 355 (2001).
[11] A. Kabla, J. Scheibert, and G. Debregeas, J. Fluid Mech. **587**, 23 (2007); **587**, 45 (2007).
[12] P. Schall, D. A. Weitz, and F. Spaepen, Science **318**, 1895 (2007).
[13] A. Amon, V. B. Nguyen, A. Bruand, J. Crassous, and E. Clément, Phys. Rev. Lett. **108**, 135502 (2012).
[14] A. Le Bouil, A. Amon, S. McNamara, and J. Crassous, Phys. Rev. Lett. **112**, 246001 (2014).
[15] C. E. Maloney and A. Lemaître, Phys. Rev. E **74**, 016118 (2006).
[16] A. Tanguy, F. Leonforte, and J.-L. Barrat, Eur. Phys. J. E **20**, 355 (2006).

[17] P. Chaudhuri and J. Horbach, Phys. Rev. E **88**, 040301 (2013).
[18] M. Cloitre, R. Borrega, and L. Leibler, Phys. Rev. Lett. **85**, 4819 (2000).
[19] C. Derec, G. Ducouret, A. Ajdari, and F. Lequeux, Phys. Rev. E **67**, 061403 (2003).
[20] V. B. Nguyen, T. Darnige, A. Bruand, and E. Clément, Phys. Rev. Lett. **107**, 138303 (2011).
[21] M. Siebenbürger, M. Ballauff, and Th. Voigtmann, Phys. Rev. Lett. **108**, 255701 (2012).
[22] P. Debenedetti and F. Stillinger, Nature (London) **410**, 259 (2001).
[23] A. Nicolas, K. Martens, and J.-L. Barrat, Europhys. Lett. **107**, 44003 (2014).
[24] E. Agoritsas, E. Bertin, K. Martens, and J.-L. Barrat, Eur. Phys. J. E **38**, 71 (2015).
[25] T. Voigtmann, in *Proceedings of the Fourth International Symposium on Slow Dynamics in Complex Systems*, edited by M. Tokuyama and I. Oppenheim, AIP Conf. Proc. No. 1518 (AIP, New York, 2013), p. 94.
[26] C. Derec, A. Adjari, and F. Lequeux, Faraday Disc. **112**, 195 (1999).
[27] S. Murayama, K. Michihiro, and T. Sakagami, Soils Found. **24**, 1 (1984).
[28] P. Johnson and X. Jia, Nature (London) **437**, 871 (2005).
[29] A. Negi and C. Osuji, Europhys. Lett. **90**, 28003 (2010).
[30] L. Berthier, J.-L. Barrat, and J. Kurchan, Phys. Rev. E **61**, 5464 (2000).
[31] D. Espíndola, B. Galaz, and F. Melo, Phys. Rev. Lett. **109**, 158301 (2012).
[32] E. J. Hinch, *Perturbation Methods* (Cambridge University Press, Cambridge, 1991).
[33] S. Dagois-Bohy, B. P. Tighe, J. Simon, S. Henkes, and M. van Hecke, Phys. Rev. Lett. **109**, 095703 (2012).
[34] G. Combe and J.-N. Roux, Phys. Rev. Lett. **85**, 3628 (2000).
[35] T. Divoux, Papers Phys. **2**, 020006 (2010).
[36] T. Voigtmann, Curr. Opin. Colloid Interface Sci. **19**, 549 (2014).
[37] Ph. Marchal, N. Smirani, and L. Choplin, J. Rheol. **53**, 1 (2009).
[38] K. Nichol, A. Zanin, R. Bastien, E. Wandersman, and M. van Hecke, Phys. Rev. Lett. **104**, 078302 (2010).
[39] K. A. Reddy, Y. Forterre, and O. Pouliquen, Phys. Rev. Lett. **106**, 108301 (2011).
[40] K. Kamrin and G. Koval, Phys. Rev. Lett. **108**, 178301 (2012).
[41] D. L. Henann and K. Kamrin, Phys. Rev. Lett. **113**, 178001 (2014).
[42] O. Pouliquen and Y. Forterre, Philos. Trans. R. Soc. London Ser. A **367**, 5091 (2009).
[43] M. Bouzid, M. Trulsson, P. Claudin, E. Clement, and B. Andreotti, Phys. Rev. Lett. **111**, 238301 (2013).
[44] A. Pons, T. Darnige, J. Crassous, E. Clément, and A. Amon, Soft Matter (to be published).